INTERNATIONAL JOURNAL OF INTEGRATED ENGINEERING
ISSN: 2229-838X e-ISSN: 2600-7916

IJIE

Vol. 16 No. 9 (2024) 143-155
https://publisher.uthm.edu.my/ojs/index.php/ijie

Structural Evaluation of Timber-Concrete Composite Floor Constructed Using Open Web Truss Joist Made of LVL *Paraserianthes falcataria*

Ali Awaludin[1]*, Urwatul Wusqo[2], Rusgiyanto[1]

[1] *Department of Civil and Environmental Engineering, Universitas Gadjah Mada, Jl Grafika 2, Yogyakarta, 55281, INDONESIA*
[2] *Civil Engineering Department, Bandung State Polytechnic, Jl Gegerkalong Hilir, Bandung, 40559, INDONESIA*

*Corresponding Author: ali.awaludin@ugm.ac.id
DOI: https://doi.org/10.30880/ijie.2024.16.09.011

Article Info

Received: 17 March 2024
Accepted: 4 October 2024
Available online: 4 December 2024

Keywords

Creep, open web truss joists, Paraserianthes falcataria, TCC floors

Abstract

The adoption of LVL (laminated veneer lumber) technology is significantly improving the potential application of Sengon wood species as structural components in buildings. Therefore, this study aimed to construct and evaluate the load-bearing capacity of two timber-concrete composite floors using open web truss joist (OWTJ) made from LVL Sengon and a 60-mm thick of concrete slab, along with a timber floor without concrete as control. All floors shared a common dimension, measuring 6460 mm length, and 1000 mm in width. The non-composite (floor A) had a depth of 600 mm, while floors B and C had 660 mm, including 60-mm thick of concrete slab. In floor B, slab above OWTJ was constructed with cast-in-situ concrete, whille C was prefabricated and connected through 5/16 inch-diameter screws. All floors were subjected to a distributed water loading to 300 mm height (equals to 3kN/m^2), while floor A passed through creep test for a duration of 14 days. The results showed that floor deflection of all specimens was less than the allowable limits required by the design standards (1/360 of the floor length). Floor B yielded the smallest deflection at 3.82 mm, which was slightly higher compared to the predictid value by the numerical model (3.67 mm). Actual strain measurement through strain-gauge at some locations of floor B verified by the numerical model showed that both concrete slab and members of OWTJ were stressed below the maximum stresses. The results positively supported the new application area of LVL made from Sengon wood species in structural components, particularly as open web truss joist of Timber-Concrete Composite (TCC) floor system.

1. Introduction

Sengon wood (*Paraserianthes falcataria*) is a fast-growing species widely distributed across various locations in Indonesia including industrial plantations and forest-owned communities. This timber species is commonly harvested after 6 to 8 years of planting with an average density of 230-500 kg/m^3 at 12-15% water content [1], [2]. Currently, it is used for different purposes such as veneers, plywood, pulp and paper, packaging and pallets, and other components of light constructions. Due to its low to moderate density, Sengon timber does not have robust mechanical properties. Therefore, modifying Sengon timber in the form of engineered wood products, especially in the form of Laminated Veneer Lumber (LVL) would enhance its mechanical properties, allowing for

wider application. The previous study showed an increase in engineering properties when Sengon wood was transformed into LVL (laminated veneer lumber) products [3]. This improvement makes LVL Sengon a great potential application for structural components in buildings, contributing positively to environmental impact through the use of timber as a renewable material with greenhouse gas offsetting capabilities.

As a material for flooring systems, timber provides both advantages and disadvantages, such as a high strength-to-weight ratio, that building engineers should consider. According to laboratory tests, timber floors supported by box-section LVL Sengon joist reached 18.75 kN/m^2, which is suitable for residential constructions [4]. Furthermore, timber floors are capable of providing excellent dynamic performance. Timber floors consisting of LVL beams have a first-mode fundamental frequency exceeding 8 Hz that accomplishes the vibration limit, ensuring comfort standards for occupants [5]. However, timber floors have several disadvantages in terms of economic and durability. Despite the relatively high cost, the estimated "ready-to-assemble" cost is not significantly different compared to concrete floors [6]. In terms of durability, timber floors are very susceptible to changes in environmental conditions leading to swelling and shrinkage [7]. An innovative method that can be adopted to resolve this issue is the combination of timber joists with concrete slabs to increase capacity and protection from external changes such as environmental conditions.

The use of timber-concrete composite (TCC) floors has gained popularity in recent decades, surpassing traditional timber flooring systems. TCC floors offer various advantages, including environmental friendliness, cost competitiveness [8]–[11], and superior bearing capacity performance [12]. Generally, TCC floors consist of concrete slab supported by timber elements, which are connected by shear connectors such as lag screw, dowels, nails, or through notched-connected systems. Structural design as a lightweight floor system considers both serviceability limit states (controlling deflection and vibration) and ultimate limit states (bearing capacity) as well as fire resistance performance [7]. Related to its serviceability limit states, previous study shows that at the equivalent applied load (the total of live load and dead load), the TCC floor has 28% lower deflection than the timber floor produced from only CLT member [13]. Furthermore, other investigation on the dynamic performance of TCC floor shows that TCC floors with spans of 4.2 meters and 5.8 meters had natural frequencies of 17 Hz and 10 Hz respectively, which are greater than 8 Hz [14], [15], indicating the absence of discomfort due to vibration.

TCC floors in ultimate limit state possess a higher strength-to-weight ratio than conventional concrete floors [15], [16]. A study focusing on overhanging TCC floors with a length-to-depth ratio of 6 showed that the ultimate bearing load of the proposed floor was 5 times more than the design load for residential buildings [17]. Previously, a 7-meter prefabricated TCC floor was tested under 4 distributed line loads perpendicular to the longitudinal direction of the slab. However, this floor system collapsed at the load level of 84 kN/m^2, which is significantly above the design limit for common structures [5]. TCC floors have also shown ease in demounting and upgrading existing timber floors without the need for demolition [18], [19]. Specifically, 3.4 meters of span reached a bearing load capacity of 15.7 kN/m^2, approaching a fully composite state [19].

The evaluation of bearing load capacity of a prefabricated TCC floor using an open web truss joist made of LVL *Paraserianthes falcataria* was also reported through laboratory tests [20]. The floor was loaded using a four-point configuration with a length of 2100 mm and an open web truss joist height of 460 mm, including a 60 mm thick concrete layer at the top. The structure experienced a buckling failure and veneer delamination at a maximum bearing load of 21.19 kN/m^2. Lag screw, serving as shear connectors, showed a minimal lateral deformation, indicating a low level of composite degree. Further examination of the structural performance of this prefabricated TCC floor system is required using a uniform loading configuration and a longer floor span. Thus, this study aimed to examine the load-bearing capacity of the proposed TCC floor under uniform load. The stress-strain appeared on concrete and LVL was also investigated during the loading test. Additionally, assessing the load-deflection behaviour for a longer period would consider the creep phenomenon in the evaluation. The findings of this study are expected to provide valuable information regarding the use of LVL Sengon in the construction industry. This will support the broader adoption of LVL Sengon across various industrial applications in the future.

2. Materials and Methods

2.1 Design and Fabrication of Timber-concrete Composite Floor

Open Web Truss Joists (OWTJ) shown in Figs. 1 and 2 consist of horizontal (top and bottom chords), vertical, and diagonal members, which are designed using LRFD concept described in the National Design Standard 2018 [21]. To enable OWTJ and concrete slab to function as composite structure, screws with a diameter of 5/16 inch and 4 inches in length were selected as the shear connector. The required screw spacing was calculated using Equations (1) and (2) found in Eurocode 5 [22].

$$EI_{ef} = \sum_{i=1}^{n} (E_i I_i + \gamma_i E_i A_i a_i^2) \quad (1)$$

Int. Journal of Integrated Engineering Vol. 16 No. 9 (2024) p. 143-155

$$\gamma_i = \left[1 + \frac{\pi^2 E_i A_i s_i}{K_i l^2}\right]^{-1} \quad (2)$$

Where i refers to the number of elements of composite floor, E is the modulus of elasticity (MoE), I is the second moment of inertia, A is the cross-sectional area, a is the distance from the center of each layer to the centroid of composite system, s is the shear connector spacing, l is the length of the joist, K is the lateral stiffness of the shear connector, and g is composite action ratio.

The OWTJ structure examined in this research comprises LVL beams made of Sengon wood (*Paraserianthes falcataria*). The production of LVL and OWTJ were carried out in the workshop building of PT. Sumber Graha Sejahtera, Jakarta. Subsequently, the manufactured components were transported to the Structural Engineering Laboratory of Universitas Gadjah Mada in Yogyakarta. The mechanical properties of LVL Sengon are presented in Table 1. All joints of OWTJ are glued joints, cold-pressed at 0.85 MPa for 120 minutes. The manufacturing process of OWTJ is shown in Fig. 1, while the geometry and section dimensions of every member of OWTJ are presented in Fig. 2 and Table 2. The design was based on the γ-method, ensuring OWTJ could bear a uniform load of 5 kN/m^2. Moreover, a detail of the design calculation is available with the authors.

Fig. 1 *Fabrication of Sengon OWTJ*

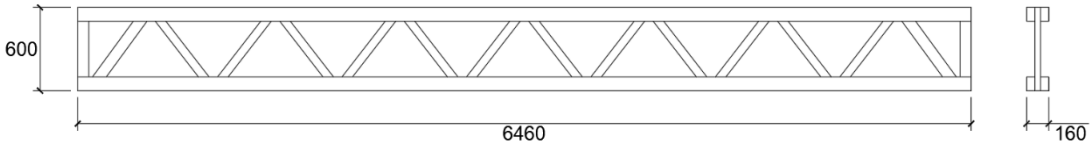

Fig. 2 *Dimension of OWTJ (units in mm)*

Table 1 *Mechanical properties of LVL Sengon [23]*

Mechanical properties	Notation	Tension (N/mm^2)	Compression (N/mm^2)
Modulus of Elasticity	E_{11}	7083	2253
	E_{22}	60.26	42.5
Poisson's ratio	u_{11}	0.225	0.225
	u_{22}	0.005	0.005
Tensile / comp. Stress	s_{u11}	46.99	25.78
Yield stress	s_{y11}	46.69	23
	s_{y22}	19.05	5.4
Shear modulus	G_{12}	919.6	919.6

Table 2 *Dimension of each member of OWTJ (units in mm)*

Top and bottom chords	Vertical member, left-most and right-most diagonal members	Diagonal members (exclude left-most and right-most members)
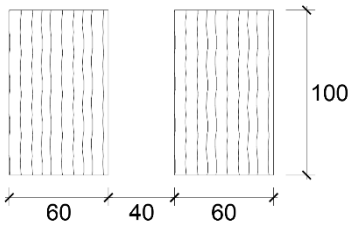	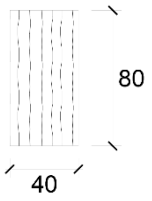	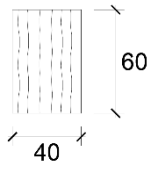

In this study, one timber floor and two timber-concrete composite specimens as described in Table 3 and Fig. 3 were fabricated. The floor dimensions were consistent across all specimens, measuring 6460 mm in length and 1000 mm in width. The non-composite (floor A) had a depth of 600 mm, while floors B and C had 660 mm including a 60 mm thick concrete slab for floors B and C. Floor A specimen is composed of two identical OWTJ with an 18-mm thick plywood connecting at the top, as shown in Fig. 3(a). Floors B and C were also the same but composed of cast-insitu and a precast concrete slab, as presented in Figs. 3(b) and 3(c). In floor C, concrete slabs were divided into 5 segments, with the dimension of 1292 mm by 1000 mm by 60 mm, and cast separately. Concrete slab has one layer of wire mesh reinforcement of 6 mm in diameter and 150 mm of spacings. Lag screw of 5/16 inch in diameter and 5 inches in length was used to transfer shear forces between concrete slab and OWTJ. Furthermore, there is a slightly different configuration in screw installation between floors B and C, due to the modular system applied on floor C. The shear connector spacing in floor C in Fig. 3(c) was arranged for the screw spacing to be located near concrete segment satisfying the minimum edge distance [24]. The total number of lag screw on floors B and C is the same, which is 180. The loading description for each floor specimen is summarized in Table 3, where only floor A was subjected to a creep test. Timber structure is sensitive to environmental changes, thus making this material vulnerable experience creep [25]. Creep phenomena become more dominant in timber than other material since timber was an organic material and hygroscopic. For this reason, the creep test only conducted on the Floor A that only consists of Open web Truss Joist covered with plywood. The applied load during the creep test was terminated after constant development of the deflection appeared.

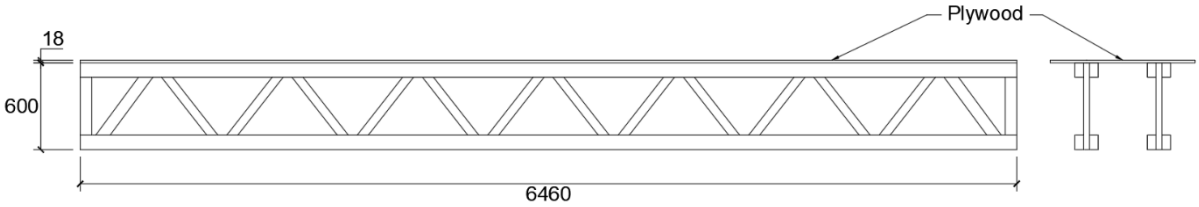

(a)

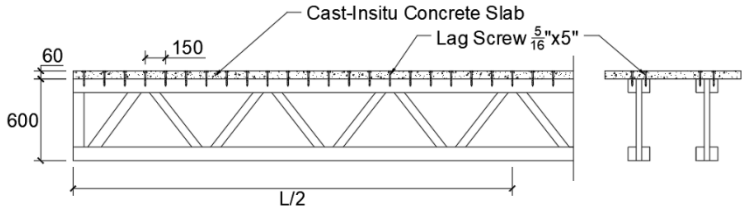

(b)

Int. Journal of Integrated Engineering Vol. 16 No. 9 (2024) p. 143-155

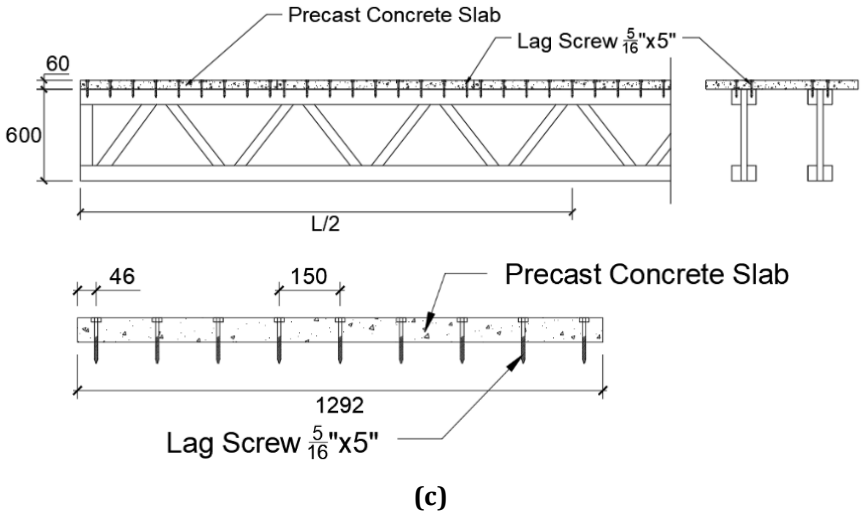

(c)

Fig. 3 *Floor system tested in this study: (a) Floor A - conventional timber floor; (b) Floor B - TCC floor cast in-situ concrete; (c) Floor C - TCC floor prefab concrete (unit in mm)*

Table 3 *Details of floor specimens*

Specimen	Floor covering type	Loading test (uniform load)		Creep test
		Loading	Unloading	
Floor A	Plywood	✓	-	✓ (14 days)
Floor B	Cast in-situ concrete slab	✓	✓	-
Floor C	Precast concrete slab	✓	✓	-

During casting of concrete slab, three samples of concrete cylinder were made. Concrete compression test after 28 days of casting showed that the average compressive strength and Young's modulus of elasticity of concrete cylinder were 19.44 MPa and 20720 MPa, respectively [26]. Subsequently, these data were applied to the numerical model developed in Section 3.

2.2 Loading Test

The floor system was subjected to a uniform-distributed load and a steel cage equipped with a water-proof sheet was placed above floor specimen to accommodate water during loading. Vertical floor deflection was measured at three different locations using linear variable displacement transducers (LVDTs, capacity 50 mm) attached to the bottom chord of OWTJ. Additionally, strain development in concrete slab and several members of OWTJ was measured using a foil-type strain gauge (SG), as shown in Fig. 4. An SG was placed at the top surface of concrete slab, while other three SG were attached to the top chord, bottom chord, and left-most diagonal member of OWTJ. The height of water inside the cage was gradually increased to 300 mm, reaching an expected uniform load of 3 kN/m^2 (total of designed live load of 2.5 kN/m^2 plus possible additional dead load of 0.5 kN/m^2). Floor deflection measurement was conducted every 50 mm increase in the water level.

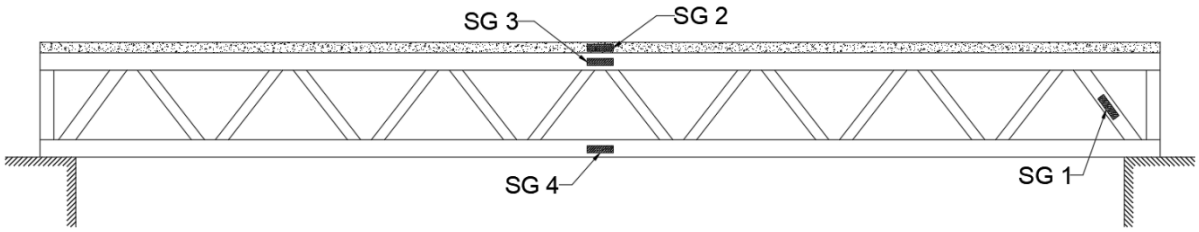

Fig. 4 *Placement of strain gauge in the specimen*

2.3 Creep Test

A creep test was conducted on floor A to examine the increase of vertical displacement caused by 14 days of loading application, as shown in Fig. 5. Although temperature and humidity inside the laboratory during the creep test were monitored, the values were not recorded. LVDT was placed in the mid-span of floor system to measure the vertical displacement, and the values obtained were recorded every 24 hours.

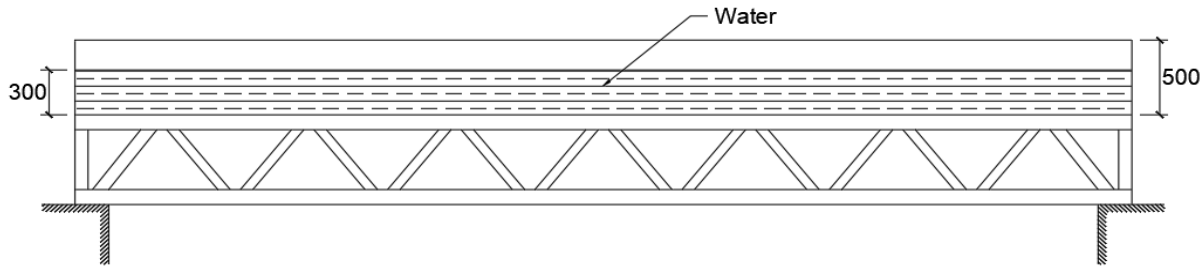

Fig. 5 *Creep test setup*

3. Numerical Analysis of Composite Floor

Fig. 6 shows the numerical model of composite floor system developed using the structural analysis software SAP 2000. Concrete slab and OWTJ components are modeled as shell and frame elements, respectively. Meanwhile, the screw connector was modeled as connecting element with constant lateral stiffness of 6.3 kN/mm, which was selected based on trial and error produced in previous studies [27]. The criterion for determining the value of constant lateral stiffness is the slope of the load-deflection curve between the results of the laboratory test and the numerical model. The mechanical properties of LVL beams and shear connectors were adopted from previous studies [24], [27]. Furthermore, the mechanical properties of concrete slab used compressive strength and modulus of elasticity obtained from concrete cylinder specimens, which were determined to be 19.44 MPa and 20720 MPa, respectively [26].

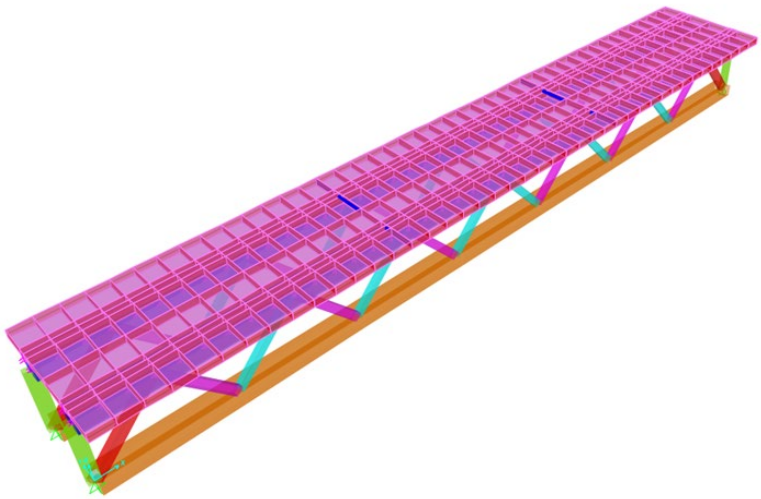

Fig. 6 *Numerical model of floor system*

Floor system was subjected to two-line loads shown in Fig. 7, for numerical model validation. The load-deflection curve obtained from the numerical analysis was compared to the experimental curve provided by previous studies [26], as shown in Fig. 8. The mid-span floor deflection of the numerical model corresponding to the applied load of 39.75 kN was found to be 9.61 mm or 7.5% lower than the experimental results of the previous research, at 10.42 mm [26]. Both load vs. deflection curves showed similar slopes at the initial stage of loading. However, experimental curves started to be non-linear at the load around 20 to 25 kN. The numerical model is good enough to capture the behavior of composite floor and can be further used to evaluate similar loads under different configurations. Fig. 9 illustrates the uniform load applied on the model for a more in-depth analysis of the composite floor.

Int. Journal of Integrated Engineering Vol. 16 No. 9 (2024) p. 143-155

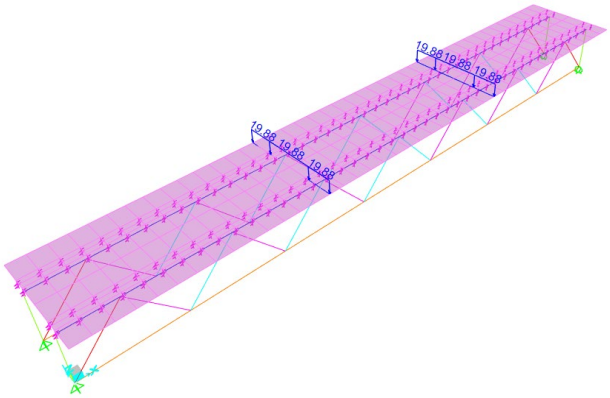

Fig. 7 *Loading scheme point loading*

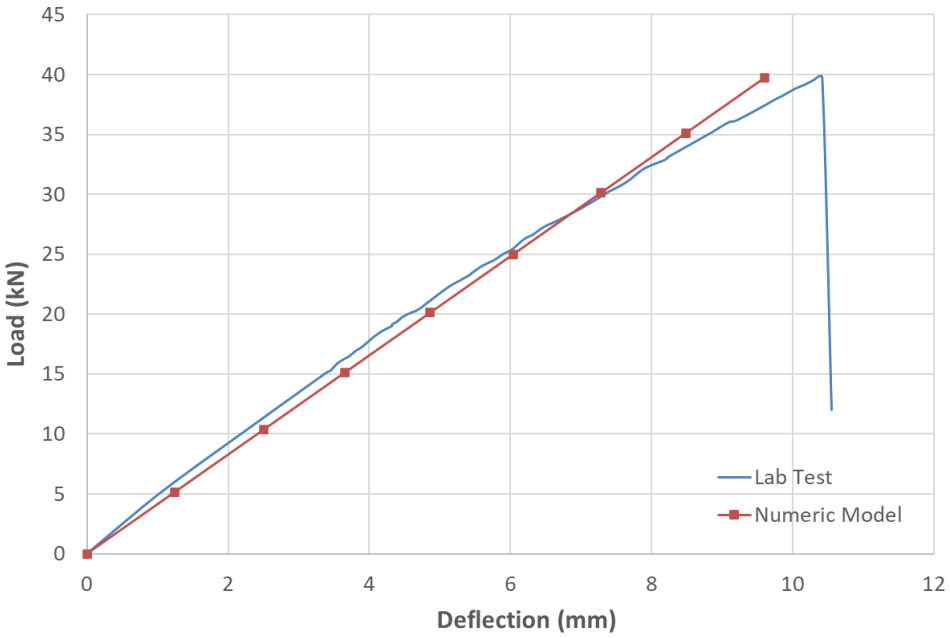

Fig. 8 *Load - deflection curve between laboratory test and numerical model*

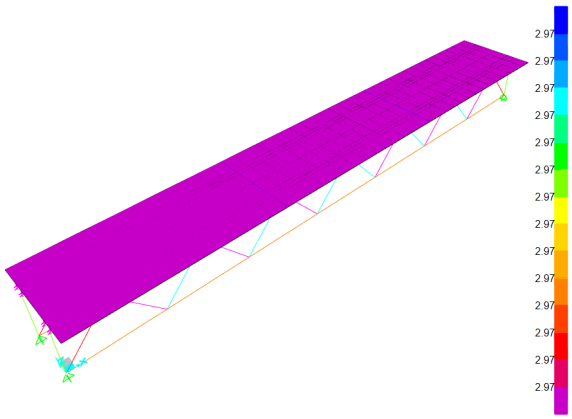

Fig. 9 *Loading scheme: distributed load*

4. Results and Discussion

4.1 Load-deflection Curve of Composite Floor

Fig. 10 shows the testing of timber-concrete composite floor, where water is continuously pumped into the steel cage to reach the targeted water level. The record of vertical displacement and axial strain measurement was conducted after a few seconds for water level stabilization. The test was continued to the next water level target and during unloading, the water was pumped out from the steel cage. Fig. 11 summarizes the vertical displacement at the mid-span of floor specimens due to distributed water loading of 300 mm height.

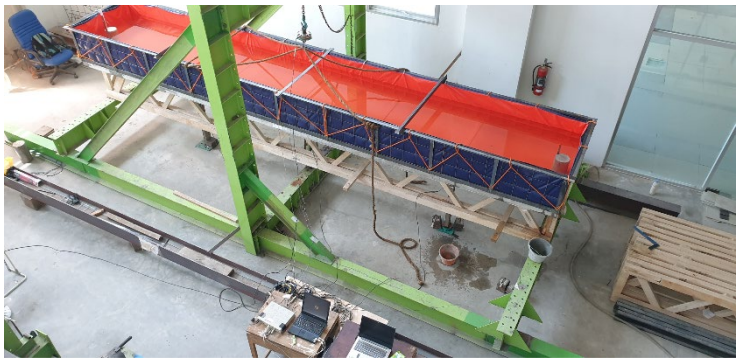

Fig. 10 *Test situation of composite floor loaded by 300 mm water height*

Fig. 11 shows the result of the loading test, indicating a total applied load of 19.2 KN on floor A, while on floors B and C was 20.825 kN including the self-weight of concrete slab. The mid-span deflection of floor A, floor B, as well as floor C was 7.35 mm, 3.82 mm, and 4.57 mm respectively. As shown in Fig. 11, the midspan deflection of floor A was highest among the other systems. Floor A produced the lowest stiffness due to the attachment of plywood with smaller stiffness value. Incorporating concrete slab in the proposed floor system significantly increased the stiffness, resulting in the reduction of the vertical deflection by more than 37%. This result showed that the vertical deflection of floor B was lower than floor C due to the use of the precast concrete system. Moreover, the precast concrete slab was made in several segments without any connecting dowels along the longitudinal axis of floor system.

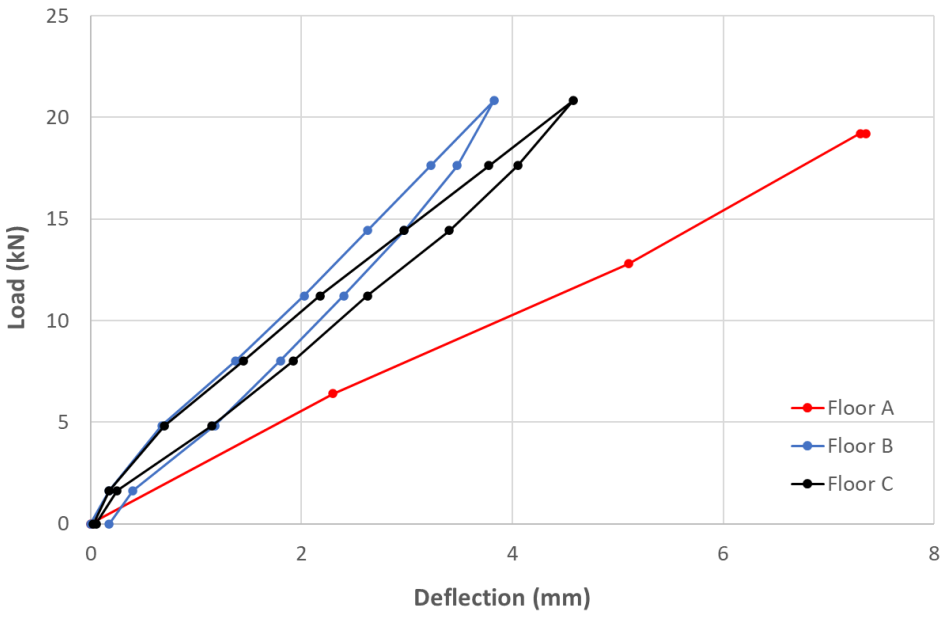

Fig. 11 *Load-deflection curve*

Int. Journal of Integrated Engineering Vol. 16 No. 9 (2024) p. 143-155

Fig. 11 shows that the maximum deflection of composite floors (floors A, B, and C) is significantly different from the standard deflection limit. According to SNI 2847:2019, the deflection limit of the floor should not exceed 1/360 of the span length or smaller than 17.94 mm [28]. Furthermore, the load-deflection curve of floors B and C during the loading-unloading process was presented, with the vertical displacement in floor system found in the elastic zone. After the water was pumped out from the steel cage, the residual displacement that occurred on floors B and C was minimal. At the same load level, the deflection during the unloading process was slightly higher than loading, showing that LVL Sengon acted as a viscoelastic material retaining a minor deformation after the stress was released.

4.2 Creep Factor

The vertical deflection of timber structures increases over time due to the creep phenomenon when subjected to a certain load level. The long-term behavior of a timber structure is mainly divided into three main phases, including primary, secondary, and tertiary creep. Since the deformation of the structure in the tertiary phase increases rapidly, some provisions provide a reduction factor for timber strength based on the service life of the structure, commonly referred to as creep factor [29]. In this research, the creep test was terminated on day 14, as there was no visible change in the measured deflection during this period. Furthermore, the creep test was conducted in the inhibited room, where the relative humidity was almost constant during the loading test, and it is fairly enough to portray the trivial change in air moisture content in Indonesia annually. Fig. 12 shows that Floor A has passed through a primary and secondary phase of creep. In the midspan (LVDT 2), a significant increase of vertical deflection occurred from day one to two of creep test, and remained constant to the conclusion of the test. The deflection in the one-third of floor span (LVDT 1 and LVDT 3) gradually increased from day one to three, without a significant change.

After 14 days of observation, the maximum deflection at LVDT 1, LVDT 2, and LVDT 3 was 5.20 mm, 7.99 mm, and 5.30 mm, respectively. In the midspan (LVDT 2), the deflection was 1.087 times the instantaneous displacement at the same location, which was smaller than creep factor provided by the Indonesian Standard (SNI 7973:2013) and NDS 2018. Both regulations require the creep factor for composite timber at 1.5 [21], [30]. Compared to previous studies, creep factor for a single OWTJ made of LVL Sengon and constantly loaded for 217 days was found to be 1.50 [31]. The numerical approach using the Prony model predicted the creep factor for the service life of 25 years at 1.57 [32]. This study provided a smaller creep factor than the regulations or the previous report, as the applied load during the 14 days of loading corresponded to a low-stress level of LVL Sengon based on the strain measurement result discussion. The deflection that occurred due to creep was highly correlated with the developed instantaneous deflection, duration of loading, and environment condition.

Creep behavior of timber-concrete composite floors was not investigated in this study. Since creep phenomenon was mainly dominant in timber material, the longer period of loading test was only conducted on floor A. Fragiacomo and Lukaszewska [33] conducted creep test on timber–concrete composite floors with prefabricated concrete slab for nearly 360 days. The result showed that during the first 240 days, as the environmental condition did not change, the mid-span deflection of timber-concrete composite floor remained fairly constant.

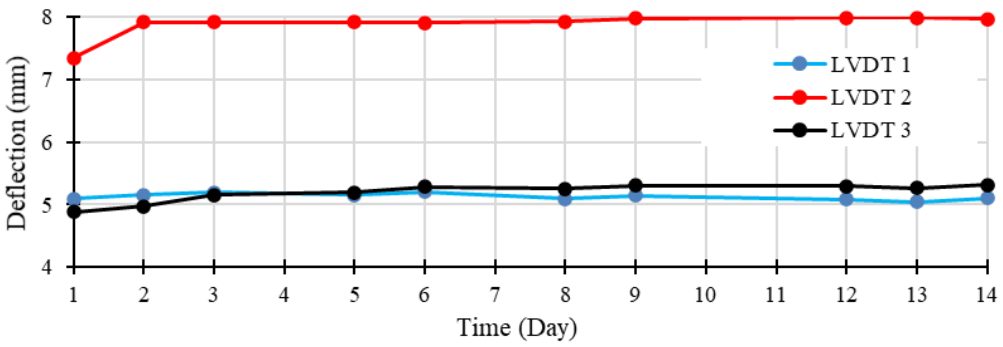

Fig. 12 *The development of vertical deflection during 14 days of load application*

4.3 Stress-strain of Composite Floor Component

The strain development during the loading test, as shown in Fig. 13, was measured using four strain gauges, located in the most-left diagonal member of OWTJ (SG1), concrete slab (SG 2), in the top (SG3), and bottom (SG4)

chord of OWTJ. The most-left diagonal member of OWTJ experienced the largest compression strain, reaching -200 x 10^{-6}. In this strain level, the diagonal member bears 1.42 MPa of compression stress. The SG2 showed that the maximum strain in concrete slab was -25 x 10^{-6}, at 0.63 MPa of compression stress. The strain on the top chord of OWTJ was approximately zero, showing that the neutral axis of floor system was around the height on the top chord of OWTJ. The maximum tensile strain occurred in the bottom chord of OWTJ, reaching 110 x 10^{-6} or tensile stress of 0.78 MPa. The stress level of both compression and tension in the LVL member is still far from its ultimate strength, which is 46.99 MPa in tension and 25.78 in compression. The comparable manner also arose on the concrete component of the floor. Furthermore, Fig. 11 shows that the strain development during the loading test remained linear, and all materials still behaved in the elastic zones. Considering the stress level along with its strain development that is within elastic zone, the proposed floor can still support loads that exceed those specified in this test (3 kN/m^2).

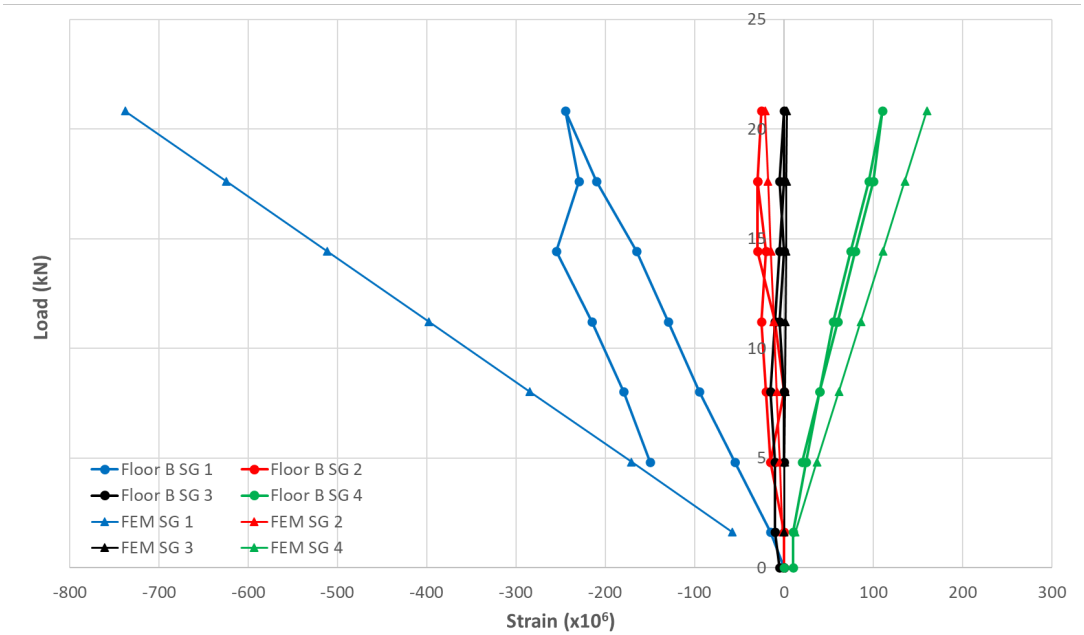

Fig. 13 *Development of a strain of the floor B during loading*

Strain development was presented alongside the actual measurements at four locations of strain gauge installation, as shown in Fig. 4 and predicted by the numerical model in Fig. 13. A significant agreement between the prediction and the actual measurement was observed, particularly in locations of SG2 and SG3. However, a significant difference was found in SG1, located in the most-left diagonal member of OWTJ, due to the non-homogeneous properties of Sengon wood as a natural product. Fig. 14 shows load-deflection curves of floor B at mid-span and quarter-span obtained from both experiment and numerical analysis. Although numerical analysis and experimental results show a substantial agreement, a noticeable difference can be observed in the initial loading stage and deflection response below 50 mm height of water loading. Floor B mid-span and quarter-span deflection corresponded to a 300 mm height of water loading was 3.67 mm and 2.72 mm, which were 4.2% and 2% lower than the experimental results.

Int. Journal of Integrated Engineering Vol. 16 No. 9 (2024) p. 143-155

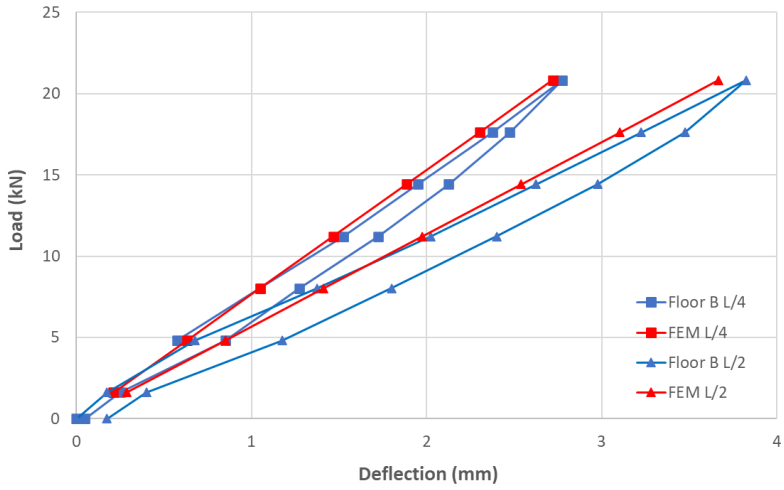

Fig. 14 *Load - deflection curve at quarter-span (L/4) and mid-span (L/2) of floor B*

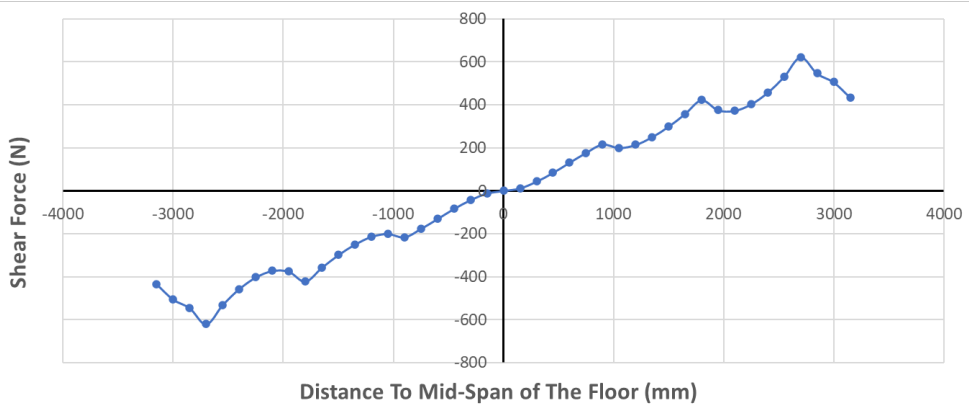

Fig. 15 *Predicted shear force for each lag screw position of floor B*

According to the results of the numerical model presented in Fig. 15, lag screw connectors passed through shear forces, which were zero at mid-span and maximum near the support of TCC floors. This distribution of shear force acting on lag screw connectors followed general understanding due to the influence on uniform distributed load. The maximum shear force was 621 N, which was relatively small compared to the maximum lateral resistance reported in the previous studies [27], [34]. Consequently, inter-layer slip between concrete slab and OWTJ caused by bending deformation of the lag screw connectors was negligible. Based on the results, further study is recommended to determine the optimum number of lag screw connectors of TCC floor system.

5. Conclusion

In conclusion, this study successfully constructed and tested composite-system floor composed of a 60-mm thick concrete slab and 600-mm height OWTJ of LVL Sengon wood species. The floor had 180 lag screws 5/16 inch, a span length of 6460 mm and was loaded by imposing uniform/distributed water load to a 300 mm height. The results showed that the mid-span deflection was 3.82 mm and 4.57 mm for cast-insitu and prefabricated concrete slabs, respectively. The values were significantly below the allowable deflection limit set by the design standard, which was 17.94 mm (1/360 of the floor span). The numerical analysis found that shear forces acting on the lag screw shear connector were relatively small, making interlayer slip between concrete slab and OWTJ negligible. Both measurement and numerical analysis results showed that compressive stress on the top surface of concrete slab and axial stresses developed in the members/components of OWTJ were significantly below the maximum values.

Acknowledgement

The authors are grateful to the Ministry of Education, Culture, Research and Technology of Indonesia for the financial support provided in this study through PTUPT program for 2019 to 2022. The authors are also grateful to PT. Sumber Graha Sejahtera for providing LVL *Paraserianthes falctaria* material during the analysis.

Conflict of Interest

Authors declare that there is no conflict of interests regarding the publication of the paper.

Author Contribution

The authors confirm contribution to the paper as follows: Ali Awaludin ***performed the study conception, research design, analysis, result interpretation, and manuscript drafting****; Urwatul Wusqo* ***conducted data collection, analysis and drafting manuscript****; and Rusgiyanto* ***conducted analysis and drafting manuscript****. All authors reviewed the results and approved the final version of the manuscript.*

References

[1] Krisnawati, H., Varis, E., Kallio, M. H. & Kanninen, M. (2011). *Paraserianthes falcataria (L.) Nielsen: Ecology, silviculture and productivity*, Center for International Forestry Research. https://doi.org/10.17528/cifor/003394

[2] Stewart, H. T. L., Race, D. H., Rohadi, D. & Schmidt, D. M. (2021) Growth and profitability of smallholder sengon and teak plantations in the Pati district, Indonesia, *Forest Policy and Economics*, *130*, 102539, https://doi.org/10.1016/j.forpol.2021.102539

[3] Awaludin, A., Shahidan, S., Basuki, A., Mohd Zuki, S. S. & Mohamed Nazri, F. (2018) Laminated Veneer Lumber (LVL) Sengon: An innovative sustainable building material in Indonesia, *International Journal of Integrated Engineering*, *10*(*1*), 17–22, https://doi.org/10.30880/ijie.2018.10.01.003

[4] Awaludin, A., Firmanti, A., Muslikh, Theodarmo, H. & Astuti, D. (2017) Wood Frame Floor Model of LVL Paraserianthes Falcataria, *Procedia Engineering*, 171, 113–120, https://doi.org/10.1016/j.proeng.2017.01.317

[5] Sartori, T. & Crocetti, R. (2016) Prefabricated timber-concrete composite floors, *European Journal of Wood and Wood Production*, 74 (3), 483–485, https://doi.org/10.1007/s00107-016-1007-4

[6] Hassan, O. A. B., Öberg, F. & Gezelius, E. (2019) Cross-laminated timber flooring and concrete slab flooring: A comparative study of structural design, economic and environmental consequences, *Journal of Building Engineering*, 26, p. 100881, https://doi.org/10.1016/j.jobe.2019.100881

[7] Bazli, M., Heitzmann, M. & Ashrafi, H. (2022) Long-span timber flooring systems: A systematic review from structural performance and design considerations to constructability and sustainability aspects, *Journal of Building Engineering*, 48, p. 103981, https://doi.org/10.1016/j.jobe.2021.103981

[8] Rodrigues, N. J., Dias, A. M. P. G. & Providência, P. (2013) Timber-Concrete Composite Bridges: State-of-the-Art Review, *BioResources*, 8 (4), 6630–6649,

[9] Lecours, L., Nguyen, T. T., Sorelli, L., Blanchet, P. & Durand, K. (2023) Optimizing composite floors for sustainability and efficiency: Cross laminated timber, concrete types, and ductile notch connectors with enhanced shape, *Cleaner Engineering Technology*, 14, p. 100635, https://doi.org/10.1016/j.clet.2023.100635

[10] Numa Bertola, Celia Küpfer, Edgar Kälin, & Eugen Brühwiler (2021) Assessment of the environmental impacts of bridge designs involving UHPFRC, *Sustainability*, 13(22), 1–19, https://doi.org/10.3390/su132212399

[11] Eslami, H., Yaghma, A., Jayasinghe, L. B. & Waldmann, D. (2023) Influence of Different End-of-Life Cycle Scenarios on the Environmental Impacts of Timber-Concrete Composite Floor Systems [Conference Session], World Conference on Timber Engineering Oslo 2023, 982–988, https://doi.org/10.52202/069179-0134

[12] Lukaszewska, E., Fragiacomo, M. & Johnsson, H. (2009) Laboratory Tests and Numerical Analyses of Prefabricated Timber-Concrete Composite Floors," *Jounal of Structural Engineering*, 136 (1), https://doi.org/10.1061/(ASCE)ST.1943-541X.000008

[13] Binder, E., Derkowski, W. & Bader, T. K. (2022) Development of Creep Deformations during Service Life: A Comparison of CLT and TCC Floor Constructions, *Buildings*, 12 (2), https://doi.org/10.3390/buildings12020239

[14] Rijal, R., Samali, B., Shrestha, R. & Crews, K. (2016) Experimental and analytical study on dynamic performance of timber floor modules (timber beams), *Construction and Building Material*, 122, http://dx.doi.org/10.1016/j.conbuildmat.2016.06.027

[15] Xie, Z., Hu, X., Du, H. & Zhang, X. (2020) Vibration behavior of timber-concrete composite floors under human-induced excitation, *Journal of Building Engineering*, 32, p. 101744, https://doi.org/10.1016/j.jobe.2020.101744
[16] Yeoh, D., Fragiocomo, M., Fransceschi, M. D. & Boon, K. H. (2010) State of the Art on Timber-Concrete Composite Structures: Literature Review, *Jorunal of Structural Engineering*, 137(10), https://doi.org/10.1061/(ASCE)ST.1943-541X.0000353
[17] Cimadevila, J. E., Riestra, F. R., Gutiérrez, E. M. & Chans, D.O. (2023) Full scale testing of timber-concrete composite floors in an overhanging configuration, *Engineering Structures*, 291, https://doi.org/10.1016/j.engstruct.2023.116460
[18] Eslami,H., Jayasinghe, L. B. & Waldmann, D. (2023) Experimental and Numerical Investigation of a Novel Demountable Timber-Concrete Composite Floor, 13, 1–19, https://doi.org/10.3390/buildings13071763
[19] Fragiacomo, M. (2012) Experimental behaviour of a full-scale timber-concrete composite floor with mechanical connectors, *Materials and Structures*, 45(11), 1717–1735, https://doi.org/10.1617/s11527-012-9869-3
[20] Awaludin, A., Wusqo, U., Setiawan, A. F., Suhendro, B., Siswosukarto, S., Basuki, A. & Leitjen, A. (2021) Structural Performance of Prefabricated Timber-Concrete Composite Floor Constructed Using Open Web Truss Joist Made of LVL Paraserianthes Falctaria, *Open Journal of Civil Engineering*, 11(04), 434–450, https://doi.org/10.4236/ojce.2021.114026
[21] American Wood Council (2018) *National Design Specification for Wood Construction*. Leesburg: American Wood Council
[22] The European Union, *Eurocode 5: design of timber structures- Part 1-1 : General- common rules and rules for buildings*, vol. 1 (2004) Brussles: European Committee for Standardization
[23] Awaludin, A., Irawati, I. S. & Shulhan, M. A. (2019) Two-dimensional finite element analysis of the flexural resistance of LVL Sengon non-prismatic beams, *Case Studies in Construction Material*, 10, https://doi.org/10.1016/j.cscm.2019.e00225
[24] Ginting, W. F. (2022) *Sistem Lantai dengan Beton Precast menggunakan Rangka LVL Sengon*. Yogyakarta: Department of Civil and Environmental Engineering, Universitas Gadjah Mada,
[25] Huang, Y. (2016) Creep behavior of wood under cyclic moisture changes: interaction between load effect and moisture effect, *Journal of Wood Science*, 62(5), 392–399, https://doi.org/10.1007/s10086-016-1565-4
[26] Chintia, A. (2021) *Kemampuan Dukung Lantai Komposit Slab Beton Cast In Situ dengan Truss LVL Kayu Sengon*. Yogyakarta: Department of Civil and Environmental Engineering, Universitas Gadjah Mada,
[27] Tantisaputri, I. A., Awaludin, A. & Siswosukarto, S. (2019) Analisa Kekuatan Tahanan Lateral Pada Sistem Komposit LVL Kayu Sengon dan Beton Pracetak, *Media Komunikasi Teknik Sipil,* 25(2) , 132–140, https://doi.org/mkts.v25i2.23068
[28] Badan Standardisasi Nasional (2019) SNI 2847-2019: Persyaratan Beton Struktural untuk Bangunan Gedung, Jakarta: Badan Standardisasi Nasional.
[29] Granello, G. & Palermo, A. (2019) Creep in timber: research overview and comparison between code provisions, *New Zealand Timber Design Journal*, 27(1), 6–22,.
[30] Badan Standardisasi Nasional (2013) *SNI 7973-2013 Spesifikasi Desain untuk Konstruksi Kayu*. Jakarta: Badan Standardisasi Nasional
[31] Basuki, A., Awaludin, A., Suhendro, B. & Siswosukarto, S. (2021) Perilaku Rangkak Open Web Truss Joist (OWTJ) LVL Sengon, *Media Komunikasi Teknik Sipil*, 27(1), 9–17, https://doi.org/mkts.v27i1.31916
[32] Basuki, A., Awaludin, A., Suhendro, B. & Siswosukarto, S (2018) Predicting bending creep of laminated veneer lumber (LVL) sengon (Paraserianthes falcataria) beams from initial creep test data, *MATEC Web of Conference*, 195, https://doi.org/10.1051/matecconf/201819502028
[33] Fragiacomo, M. & Lukaszewska, E. (2013) Time-dependent behaviour of timber-concrete composite floors with prefabricated concrete slabs, *Engineering Structures*, 52, 687–696, https://doi.org/10.1016/j.engstruct.2013.03.031
[34] Wusqo, U., Awaludin, A., Setiawan, A. F. & Irawati, I. S. (2019) Study of Laminated Veneer Lumber (LVL) Sengon to Concrete Joint Using Two-Dimensional Numerical Simulation, *Journal of Civil Engineering Forum*, 5(3), https://doi.org/10.22146/jcef.47694